RESEARCH ARTICLE

Macromolecular Materials and Engineering
Open Access
www.mame-journal.de

Phosphorus and Silicon Modified Alginate as an Efficient Flame Retardant for Poly(lactic acid)

*Kata Enikő Decsov, Viktória Cserni, Beáta Szolnoki, Olga Krafcsik, and Katalin Bocz**

The introduction of biobased carbon sources in intumescent flame retardant formulations is extensively explored, particularly for biopolymers such as poly(lactic acid) (PLA). In this work, the flame retardant efficiency of alginate, a favorable renewable charring agent candidate, is enhanced by chemical modification with a phosphorus- and silicon-containing compound and subsequent coagulation in the presence of Ca^{2+} ions. The simultaneous presence of P and Si atoms in the reactive compound is shown to be an effective way to avoid thermal stability issues related to the biobased carbohydrate. The newly synthesized PSilAlg additive boosts the flame-retardant effectiveness of ammonium-polyphosphate (APP) at low loadings. Adding 5 wt% PSilAlg to 15 wt% APP containing PLA composite increases the limiting oxygen index from 26.0 to 34.0 vol% and decreases the total heat emission during combustion by 46%, accompanied by significantly (by 66%) reduced smoke production. The outstanding flame retardant performance of PSilAlg is attributed to the high amount and thermally stable carbonaceous fire-protecting layer that forms as a result of the enhanced charring, catalyzed by the high oxidation state P, and the strengthening mechanism of inorganic silicates and calcium salts.

1. Introduction

Poly(lactic acid) (PLA) is an attractive and favorable biopolymer for engineering applications where fire safety is essential. The use of phosphorus-based intumescent flame retardants (IFRs) is one of the most promising methods for flame retardancy of PLA due to their high efficiency, low smoke production, and low toxicity.[1,2]

A commonly used IFR system is a combination of a polyphosphate salt (ammonium polyphosphate (APP) or melamine polyphosphate), acting both as an acid source and foaming agent, and a hydroxyl-rich char former such as pentaerythritol (PER). Potential synergistic effects have been reported on a large variety of substances, including zinc-borate, silica nanoparticles, tetraethoxysilane, polytetrafluoroethylene,[3] various clay minerals,[4] modified graphene oxide,[5] graphene layers,[6] metal–organic frameworks,[3] etc.

In the past, the petroleum-based PER was most often used as a charring agent to impart flame retardancy to PLA; however, an increasing number of studies are underway with the aim to replace it with a renewable, biobased alternative. For this purpose, the use of lignin and various carbohydrate derivatives came to the forefront; among others, starch, cellulose, chitin, chitosan, and alginate have already been used to increase the degree of charring and thus the flame retardant effect in PLA.[2]

Réti and his colleagues[7] measured an oxygen index of 58 vol% and a UL-94: V-2 flammability category for the PLA composite with 30 wt% APP + 10 wt% PER content. By replacing PER with 10 wt% biobased lignin or starch, limiting oxygen index (LOI) decreased to 32 and 40 vol%, respectively. However, both composites containing biobased charring agents obtained V-0 classification according to the UL-94 flammability test. Zhang et al.[8] used lignin and urea-modified lignin in addition to APP for flame retardancy of PLA. With the use of 18.4 wt% APP and 4.6 wt% lignin, an oxygen index of 33.0 vol% and a UL-94: V-2 classification were obtained, while with the same composition but using urea-modified lignin, their test samples were characterized by an oxygen index of 34.5 vol% and a V-0 rating.

Alginate is a naturally occurring anionic polysaccharide typically extracted from brown seaweed. It has vast applications in biotechnology, biomedical engineering, food processing, and pharmaceuticals. Many researchers[9–12] reported that the metal ion complexes of alginic acid exhibit inherent flame retardancy; therefore, they are potential raw materials for preparing biobased flame retardants. The flame retardancy effect of the metal-alginate complexes relies mainly on the change of the pyrolysis

K. E. Decsov, V. Cserni, B. Szolnoki, K. Bocz
Department of Organic Chemistry and Technology
Faculty of Chemical Technology and Biotechnology
Budapest University of Technology and Economics
Műegyetem rkp. 3., Budapest H-1111, Hungary
E-mail: bocz.katalin@vbk.bme.hu
O. Krafcsik
Department of Atomic Physics
Institute of Physics
Budapest University of Technology and Economics
Műegyetem rkp. 3., Budapest H-1111, Hungary

The ORCID identification number(s) for the author(s) of this article can be found under https://doi.org/10.1002/mame.202400194

DOI: 10.1002/mame.202400194

process and the generation of metal oxides and metal carbonates during combustion, which form a barrier between the flame and the condensed phase, which effectively cuts off the heat transfer, the penetration of oxygen and the spread of flammable gases.[11]

According to the recently published review on the use of alginates as flame retardant materials by Xu et al.,[13] among various polyvalent metal ions, the incorporation of Ca^{2+} provides the best flame retardancy by effectively increasing the yield and thermal stability of the char residue. In order to enhance the flame retardancy performance of metal-alginate complexes, combination with inorganic additives such as polyphosphates, metal hydroxides, silica particles, and clay minerals[14] or chemical modifications with the aim to utilize catalytic effects (such as P-induced charring) or synergistic interactions (P–N[15,16] or P–Si synergisms[17–20]), are promising ways.

Pallman et al.[21] prepared phosphorylated sodium alginate (PSA) with the aim of creating a natural-sourced IFR system for polypropylene. PSA was found to be effective in promoting char formation and smoke suppression; however, its relatively low decomposition temperature may limit its application potential as a flame retardant additive.

The shortcoming of low thermal stability was successfully overcome by Chen et al.,[22] who reacted calcium alginate with a phosphorus- and silicon-containing compound (CADPP). The CADPP additive was obtained by reacting sodium-alginate (SA) with the reactive flame retardant (DPP), derived from the reaction of 9,10-dihydro-9-oxa-10-phosphaphanthrene-10-oxide (DOPO) and γ-(2,3-epoxypropoxy) propyltrimethoxysilane (SCA),[23] followed by coagulation in $CaCl_2$ solution. CADPP was successfully used for flame retardancy of epoxy resin (EP). With 30 wt% CADPP additive, the epoxy composite achieved a UL-94: V-0 rating and an LOI of 29.3 vol%, while PHRR and HRC reduced by 60% compared to neat EP during microscale combustion calorimetry testing. The excellent flame-retardant effect of CADPP was ascribed to the advantageous combination of the self-charring capacity of alginate that is catalyzed by the P and the char-reinforcing effect of Si, which contributes to the formation of a coherent, compact, and strengthened fire-protecting layer of increased efficiency. Nevertheless, DOPO is considered to act predominantly in the gas phase by releasing PO^* and $PO_2{}^*$ radicals with a flame inhibition effect through a radical trapping mechanism.[24] In the present research, it is proposed that a compound in which the P atom is of higher valence, such as phosphates or phosphonates, would have an increased charring effect,[25] and thus it could better contribute to the formation of a protective carbonaceous layer.

The overall aim of this research work was to develop an efficient intumescent formulation for flame retardancy of PLA using alginate as a readily available and renewable starting material. In order to increase the effectiveness of calcium-alginate as a flame retardant, reactive modification with a phosphorus and silicon-containing compound was performed using additional chemical reactions. The newly synthesized additive was characterized by spectroscopic and thermal analytical methods, while its flame retardant effect was investigated in PLA matrix in addition to APP by standard flammability tests.

2. Experimental Section

2.1. Materials

Ingeo Biopolymer 4032D grade PLA (D-lactide content: 1.5%, melt flow index at 190 °C and 2.16 kg load: 9 g /10 min) was purchased from NatureWorks LLC (Minnetonka, MN, USA). ExolitAP 422 type ammonium-polyphosphate (APP) was supplied by Clariant AG (Muttenz, Switzerland). Sodium alginate (SA) and calcium dichloride were purchased from Merck Life Science Kft (Budapest, Hungary). The phosphorous silane (PSil) used for reactive modification was synthesized according to Bocz et al.[19] using 3-(triethoxysilyl)- propyl isocyanate (Merck Life Science Kft, (Budapest, Hungary)) and ExolitOP 560 phosphonate polyol (Clariant Plastics & Coatings GmbH (Frankfurt, Germany)). The toxicity risk of the isocyanate compound was minimized by following the safety datasheet's advice on safe storage and handling (work under the hood using appropriate personal protecting equipment).

2.2. Synthesis of Modified Alginate (PSilAlg)

The reaction scheme of PSilAlg preparation is presented in **Figure 1**. To prepare 3.5 wt% SA solution, 14.0 g SA was dissolved in 400 mL deionized water and kept overnight under stirring at room temperature. Then 28.0 g of PSil (weight ratio of SA:PSil = 1:2) was added dropwise to the aqueous solution of SA and uniformly mixed. The mixture was then heated to 100 °C and continually stirred for 5 h to realize etherification between PSil and alginate. After, calcium alginate beads were formed by feeding the solution dropwise into a 2 wt% calcium dichloride coagulation bath. For this, the alginate solution was transferred using a 50 mL syringe with a thin-walled needle made of stainless chrome-nickel steel using a syringe pump at a constant flow rate of 250 mL h^{-1}. The beads were cross-linked and hardened in the gelation bath for 30 min and then filtered, washed with deionized water, dried (at 80 °C for 24 h), and pulverized. An overall yield of 22% was determined for the synthetic sequence of the PSilAlg additive.

2.3. Preparation of Flame Retarded PLA Composites

PLA composites with compositions according to **Table 1** were prepared using a Brabender Plasti-Corder Lab-Station (Brabender GmbH & Co. KG, Duisburg, Germany) internal mixer. The melt-mixing was performed at 180 °C for 5 min with a rotor speed of 50 min^{-1}.

The obtained homogeneous materials were dried overnight at 80 °C and then molded into 3 mm thick plates using a Teach-Line Platen Press 200E (Dr. Collin GmbH, Munich, Germany) type hydraulic press set to 180 °C. The specimens required for flammability tests were obtained by cutting the plates with a saw.

2.4. Characterization Methods

2.4.1. Fourier Transform Infrared Spectroscopy

Infrared spectra (4000–600 cm^{-1}) werecollected using a Bruker Tensor 37 type Fourier transform infrared (FTIR) spectrometer

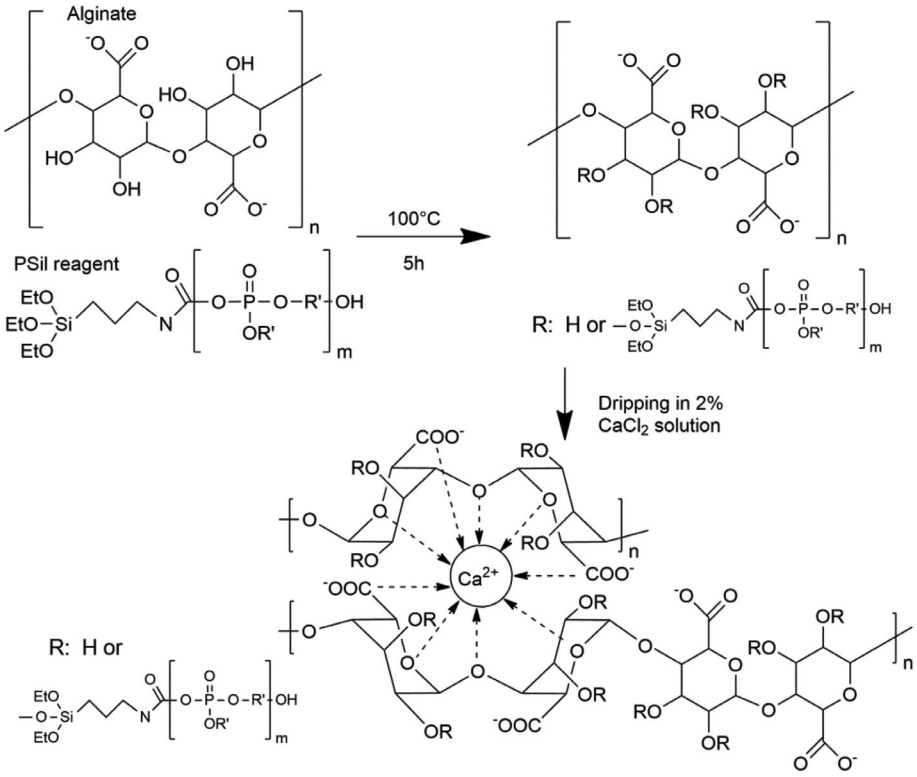

Figure 1. Preparation of PSilAlg.

(Bruker Corporation, Billerica, MA, USA) equipped with deuterated triglycine sulfate detector in attenuated total reflectance (ATR) mode with a spectral resolution of 4 cm^{-1} and 32 scan accumulation.

2.4.2. Scanning Electron Microscopy Coupled Energy Dispersive Spectroscopy

Scanning electron microscopy coupled energy dispersive spectroscopic analyses (SEM/EDS) were performed using a JEOL JSM-5500 LV type (JEOL Ltd., Akishima, Tokyo, Japan) apparatus. Elemental mapping was carried out with an accelerating voltage of 15 keV and an amplification of ×1300.

2.4.3. X-Ray Photoelectron Spectroscopy

The X-ray photoelectron spectroscopy (XPS) measurements were carried out using a twin anode X-ray source (Thermo Fisher Scientific, Waltham, MA, USA, XR4) and a hemispherical energy analyzer with a nine-channel multi-channeltron detector (SPECS-GROUP, Berlin, Germany, Phoibos 150 MCD). The base pressure of the analysis chamber was $\approx 2 \times 10^{-9}$ mbar. Samples were analyzed using a Mg K_α (1253.6 eV) anode without monochromatization.

Table 1. Formulations of the PLA composites.

Sample name	PLA [wt%]	APP [wt%]	PSilAlg [wt%]
PLA	100	–	–
PLA_APP	85	15	–
PLA_APP_1PSilAlg	84	15	1
PLA_APP_3PSilAlg	82	15	3
PLA_APP_5PSilAlg	80	15	5

2.4.4. Thermogravimetric Analysis

Thermogravimetric analyses (TGA) were performed using a TA Instruments Q5000 apparatus (TA Instruments LLC, New Castle, NH, USA). Samples of 5–8 mg were placed in platinum pans and heated from room temperature to 600 °C at a 10 °C min^{-1} rate under a nitrogen gas flow of 25 mL min^{-1}. Before starting the measurement program, the additives were dried in the apparatus for 10 min at 120 °C under a nitrogen gas flow of 25 mL min^{-1} and then cooled back to room temperature without opening the apparatus.

2.4.5. Limiting Oxygen Index

Limiting oxygen index (LOI) measurements were performed on 3 mm thick specimens according to the ISO 4589 standard using a Fire Testing Technology Ltd. (East Grinstead, UK) apparatus.

2.4.6. UL-94 Test

The UL-94 standard flammability tests were carried out on 3 mm thick specimens according to ASTM D3081 and ASTM D635 standards.

2.4.7. Pyrolysis Combustion Flow Calorimetry

Pyrolysis combustion flow calorimetry (PCFC) measurements were performed on a Fire Testing Technology FAA Micro Calorimeter (FTT, United Kingdom) type apparatus. The applied heating rate was 1 °C sec^{-1}, the combustion temperature was 900 °C, and the maximum pyrolysis temperature was 750 °C. About 4–5 mg of sample was used in each test.

2.4.8. Cone Calorimetry

Cone calorimetry tests were carried out using a TCC 918 (Netzsch, Germany) type instrument according to the ISO 5660–1 standard. Samples of 100 × 100 × 3 mm^3 dimensions were exposed to a constant heat flux of 35 kW m^{-2}. The main combustion characteristics, such as the heat release rate (HRR) as a function of time, the time to ignition (TTI), the total heat release (THR), and the peak of heat release rate (PHRR), mass loss rate (MLR), smoke production rate (SPR), total smoke production (TSP) and residual mass were obtained. From these data, the maximum average rate of heat emission (MARHE) and the flame retardance index (FRI)[26] (according to Equation (1)) were calculated. The measurements were performed in duplicate where the PHRR values were reproducible within ±10% while THR values were within ±5%.[26]

$$FRI = \frac{\left[\left(\frac{PHRR}{TTI}\right) \times THR\right]_{neat\ polymer}}{\left[\left(\frac{PHRR}{TTI}\right) \times THR\right]_{composite}} \quad (1)$$

2.4.9. Raman Spectroscopy

Raman spectra were recorded using a LabRAM (Horiba Jobin Yvon) instrument. Raman excitation was performed with a 40 mW, $\lambda = 532$ nm (Nd-YAG) laser beam focused through a 20× objective. D1 filter was used to decrease excitation beam intensity reducing the chance of sample degradation. The Raman spectra were acquired using an acquisition time of 20 s and averaging 3 measured spectra at each measured point with a resolution of 2 cm^{-1}. LabSpec 6 software was applied for data collection and parameter optimization.

3. Results and Discussion

3.1. Characterization of PSilAlg

3.1.1. ATR-IR Spectroscopy

Figure 2 shows a comparison of the IR spectra of the calcium complexes of original (Alg) and PSil-modified (PSilAlg) alginates. In the spectrum of neat calcium alginate (Alg), the stretching vibrations of OH at 3250 cm^{-1} and aliphatic CH_2 at 2928 cm^{-1}, the peaks attributed to asymmetric and symmetric vibrations of the carboxylate group at 1628 and 1431 cm^{-1}, the bands corresponding to C—O vibration of the pyranose ring at 1082 cm^{-1}, and C—O—C vibration of the glycosidic bonds at 1026 cm^{-1}

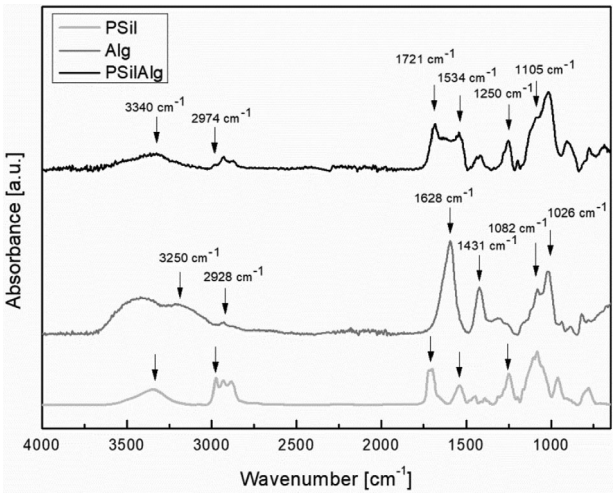

Figure 2. ATR-IR spectra of PSilAlg.

can be identified, respectively. In the spectrum of the PSil-treated alginate, the peaks assigned to the COO^- group (at 1628 and1431 cm^{-1}) become less intense, while new peaks characteristic for the phosphorous silane treating agent appear with high intensity, such as the P═O band at 1250 cm^{-1}, and bands related to the absorbance of a carbamate linkage (C═O at 1721 cm^{-1} and N—H at 1534 and 3340 cm^{-1}), besides the C—H absorption bands of CH_3 groups at 2974 cm^{-1} and additional CH_2 groups at 2928 cm^{-1}. The shoulder at 1105 cm^{-1} in the spectrum of PSilAlg is attributed to the overlap of the stretching vibration peaks of the C—O bond of the alginate and the Si—O—C bond of the adduct. The ATR-IR analysis confirms the successful etherification between PSil and the alginate and indicates a significant amount of PSil in the cross-linked structure of the product.

3.1.2. Elemental Analysis

The chemical composition of the synthesized PSilAlg additive was examined by XPS and EDS, respectively. The elemental contents obtained by the two analytical methods are compared in **Table 2**. The noticeable difference in the relative contents of the N, Ca, Si, and P elements indicates a preferred orientation of the macromolecule. Considering that XPS is a surface-sensitive technique, it can be assumed that the siloxane and carbamate linkages likely orient outward, while the Ca^{2+} ion is complex and oriented toward the interior of the polysaccharide ring.

Table 2. Elemental composition of PSilAlg according to XPS and EDS analyses.

	Content [at.%] based on XPS	Content [at.%] based on EDS
C	57.3	54.7
O	28.6	37.4
N	5.3	0.0
Ca	0.8	2.5
Si	7.8	5.0
P	0.2	0.4

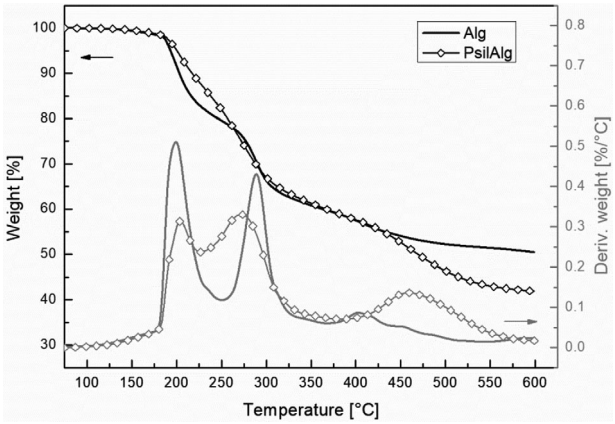

Figure 3. TG and DTG curves of Alg and PSilAlg.

Considering the P-content based on EDS that is more suitable for bulk analysis, the graft ratio of PSil on Alg is ≈15%. Nevertheless, based on the higher Si to P ratio, detected by both analytical techniques, than expected based on the theoretical chemical composition of the PSilAlg adduct, it is assumed that partial hydrolysis of the carbamate linkage may occur during the 5 h boiling in the aqueous medium during synthesis, resulting in a phosphorus-free aminosilane-grafted alginate proportion in the mixture.

3.1.3. Thermogravimetric Analysis

TG and DTG curves of the calcium complexed alginate (Alg) and its PSil-modified derivative (PSilAlg) can be seen in **Figure 3**, while the thermogravimetric analysis data are summarized in **Table 3**. The thermal decomposition of polysaccharides commonly occurs in four steps: release of absorbed water, dehydration, depolymerization, and aromatization or charring. In Figure 3, three main degradation stages can be distinguished; the weight loss due to desorption of physically absorbed water is minimal in this case since the thermal analyses were performed on pre-dried samples. It was done, considering that the additives were later used in this pre-dried form for the production of composites to reduce the risk of hydrolytic degradation of PLA during melt-processing. Nevertheless, the water uptake of the alginate samples stored under ambient conditions was also compared using TGA (Table 3). Accordingly, noticeably decreased moisture absorption was measured for the PSil-modified alginate, which can be attributed to the increased hydrophobicity of the groups (ether, alkyl, siloxane, etc.) introduced into the molecular structure of the alginate during the reactive modification. The volatilization of structural water occurs in the same temperature range of 180–220 °C for the two alginate samples; however, the weight loss is noticeably lower for the alginate modified with PSil, where some of the hydroxyl groups were converted into ether linkages. The weight loss in the temperature range of 220–330 °C is mainly related to the cleavage of glycoside bonds, and the ether and ester bonds of the PSilAlg are also destroyed in this temperature range, resulting in higher weight loss (Δm_2 = 25.4%) in this degradation step. The final decomposition step starts above 380 °C, where the formation of aromatic and graphitic structures and also calcium salts takes place. The rate of decomposition and the corresponding weight loss is noticeably higher in the case of the PSilAlg, which indicates that the phosphorus-silane modification greatly changes the degradation pathway of Alg, and upon heating, different intermediate products form at high yields. The char yield at 600 °C is as high as 50.5 and 41.9% for neat and PSil-modified alginate, respectively. The high yield of the carbonaceous residue is likely associated with the calcium ion-promoted cross-linking and cyclization reactions and the formation of calcium carbonates, while in the case of PSilAlg, the catalytic effect of P on carbonization and the Si-induced ceramisation also enhances the barrier properties of the char. According to EDS analyses, the unmodified alginate can complex a larger amount of Ca^{2+} ions (3.0 ± 0.4 at%) than the PSil-modified Alg (2.3 ± 0.7 at.%), and thus, the promoted formation of inorganic salts may explain the higher amount of residue obtained at 600 °C for Alg compared to PSilAlg.

Table 3. Thermal characteristics of Alg and PSilAlg.

		Alg	PSilAlg
stage 0	water uptake [%][a)]	16.0	9.6
stage 1	$T_{95\%}$ [°C]	193	200
	T_{onset1}	180	182
	T_{max1} [°C]	199	204
	slope1 [% °C^{-1}]	0.511	0.313
	Δm_1 [%]	20.2	10.7
stage 2	T_{onset2}	261	229
	T_{max2} [°C]	289	271
	slope$_2$ [% °C^{-1}]	0.431	0.330
	Δm_2 [%]	17.6	25.4
stage 3	T_{onset3}	381	402
	T_{max3} [°C]	403	459
	slope$_3$ [% °C^{-1}]	0.086	0.137
	Δm_3 [%]	5.1	15.9
	Residue (at 600 °C) [%]	50.5	41.9

[a)] derived from a TGA run without a pre-drying step

3.2. Characterization of Flame Retarded PLA Composites

3.2.1. Thermogravimetric Analysis

TGA curves of the flame retarded PLA composites and corresponding data are presented in **Figure 4** and **Table 4**, respectively. Based on the temperatures read at 95% mass ($T_{95\%}$), it can be concluded that the thermal stability of PLA did not decrease under the influence of the used flame retardants and even increased slightly. It is also visible that the residual mass measured at 600 °C increases with the amount of PSilAlg. In the case of the PLA composite containing 15 wt% APP and 5 wt% PSilAlg additive, ≈10% of the initial sample mass remained, which indicates the formation of a thermally stable carbonaceous structure.

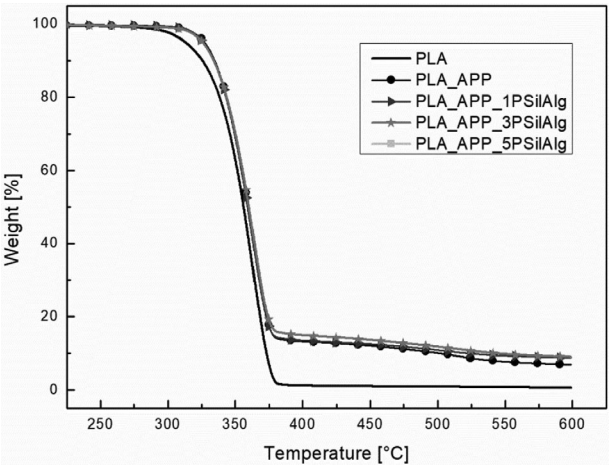

Figure 4. TGA curves of the flame retarded PLA composites.

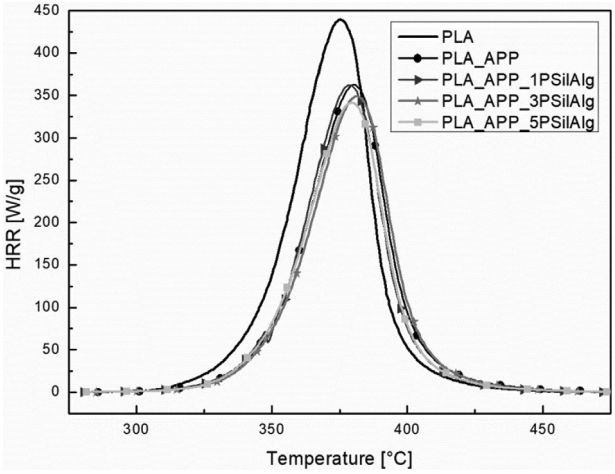

Figure 5. HRR curves of the flame retarded PLA composites.

3.2.2. Pyrolysis Combustion flow Calorimetry

Figure 5 and **Table 5** show the results obtained from the PCFC test. With increasing PSilAlg content in the PLA composites, a decrease in the peak of heat release rate (PHRR), heat release capacity (HRC), and total heat release (THR) can be seen. The PHRR value of PLA was reduced by ≈20% with flame retardant systems by including 3 or 5 wt% PSilAlg additive. It can also be established that – in accordance with the TGA results (Table 4) – the mass remaining at the end of the measurement increased proportionally with the increase in the amount of PSilAlg. While the residual mass was 0.3% in the case of neat PLA, and 7.2% remained from the composite containing 15 wt% APP, the amount of residue increased significantly to 11.4%, when 15 wt% APP was combined with 5 wt% PSilAlg additive. Accordingly, the total amount of heat emitted also decreased significantly by ≈20% when 5 wt% PSilAlg was used, from 17.0 to 13.4 kJ g^{-1}. Based on the microcalorimetric analyses, the phosphorus, and silicon-modified alginate compound was suggested to effectively fulfil the role of the carbonizing component in addition to APP.

Table 5. Results obtained from PCFC measurements.

	HRC [J gK^{-1}]	PHRR [W g^{-1}]	THR [kJ g^{-1}]	T_{PHRR} [°C]	Char yield [%]
PLA	449	439	17.0	375	0.3
PLA_APP	367	362	14.4	380	7.2
PLA_APP_1PSilAlg	369	362	14.0	379	8.7
PLA_APP_3PSilAlg	354	349	14.0	381	7.8
PLA_APP_5PSilAlg	347	342	13.4	380	11.4

3.2.3. UL-94 and LOI Test

In the standard UL-94 flammability test, the examined PLA composite samples achieved similar results; the flame went out in all cases, but the falling flaming droplets ignited the cotton wool placed underneath the specimens. So, all the composites can be classified as V-2 according to UL-94 (**Table 6**), which means a moderate level of resistance to ignition. In the case of the specimens with PSilAlg content of 3 and 5 wt%, the flaming drops leave from the bulk material immediately, which indicates reduced melt viscosity of these samples. Based on the research results of Yu et al.,[27] for PLA composites with lower melt viscosity, less flame retardant is required to pass a UL-94 V-0 rating. They claimed that specimens with lower melt viscosity start to drip earlier, which is accompanied by lower temperatures of the burning front, leading to cooled droplets before reaching the underlying cotton. In our case, the use of metal-containing flame retardant may cause degradation of PLA, but the degree of degradation is apparently not so significant to reach the critical viscosity range, which could promote early melt dripping at decreased

Table 4. Thermal characteristics of the flame retarded PLA composites.

Sample name	$T_{95\%}$ [°C]	T_{max} [°C]	slope [% $°C^{-1}$]	Residue (at 600 °C) [%]
PLA	313	363	−2.6	0.6
PLA_APP	327	364	−2.4	6.9
PLA_APP_1PSilAlg	326	363	−2.4	8.7
PLA_APP_3PSilAlg	326	364	−2.4	9
PLA_APP_5PSilAlg	322	366	−2.4	9.9

Table 6. UL-94 classification and LOI of the flame retarded PLA composites.

	LOI	UL-94	
	[vol%]	rating	total flaming time[a] [s]
PLA	21.5	HB (v_{flame} = 25.6 mm min^{-1})	
PLA_APP	26.0	V-2	13
PLA_APP_1PSilAlg	26.0	V-2	4
PLA_APP_3PSilAlg	29.0	V-2	0
PLA_APP_5PSilAlg	34.0	V-2	0

[a] 10 flame applications

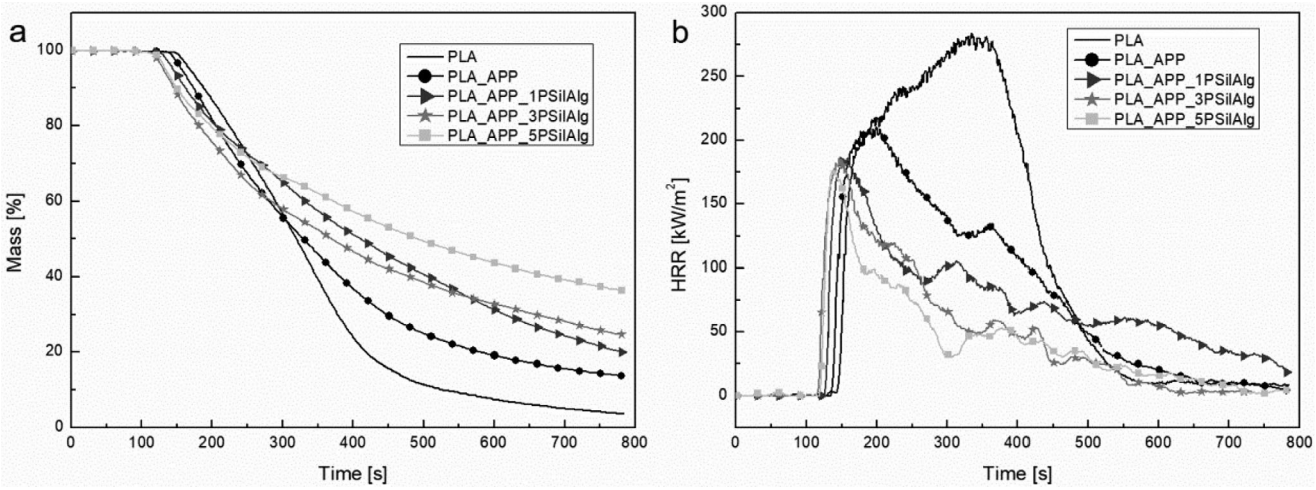

Figure 6. a) Heat release rate and b) mass loss curves of the flame retarded PLA composites.

temperature of the burning font and thus help extinguish the flame.

According to the limiting oxygen index measurements (Table 6), the addition of 1% PSilAlg to 15 wt% APP shows no difference compared to the composite containing only 15 wt% APP. However, the composite sample with 3 wt% PSilAlg additive reached a noticeably higher oxygen index of 29 vol%, while the burning of the PLA composite was self-sustaining only in an atmosphere with minimum oxygen content of 34 vol% when 5 wt% PSilAlg was used. It has to be noted that this outstandingly high oxygen index value was reached with noticeably lower amounts (only 20 wt%) of additives than in previous research works also targeting the use of biobased FR components.[7,28–31]

3.2.4. Cone Calorimetry

The HRR and MLR curves of the flame retarded PLA composites recorded during cone calorimeter tests are presented in **Figure 6**, while the evaluated combustion characteristics are listed in **Table 7**. The TTI of the flame-retardant-containing samples is shorter than that of neat PLA, which is a well-known consequence of phosphorus compounds initiated char formation,[32] which causes quick temperature rise and rapid decomposition of PLA on the upper layers of the samples. The HRR curve of the neat PLA (Figure 6a) is typical for non-charring samples, while the shape of the HRR curves of the flame-retardant-containing samples indicates considerable residue formation.[33] After ignition, there is a sharp increase in HRR values of the flame retardant samples until a carbonaceous fire-protecting layer is developed, then, the HRR values continually decrease with time until the flameout. As a result of this flame retardant mechanism, the PHRR is reached at the beginning of the combustion process. In connection to this, it can be observed that by adding 15 wt% APP, the PHRR of PLA reduced by 26%; however, this maximum was reached noticeably, 135 s faster than that in the case of neat PLA. The addition of PSilAlg at as low as 1–5 wt% to the system resulted in a further reduction of both PHRR and $PHRR_{time}$ values, which indicate char promoting effect of this compound. Compared to the total heat emission during the combustion of neat PLA (76.5 MJ m^{-2}), 15 wt% APP reduced the THR by 30%. Adding 3 wt% of PSilAlg resulted in a THR reduction of 57%, and with only 20 wt% additive content (15 wt% APP + 5 wt% PSilAlg), even 62% less heat was emitted. Similar trends can be observed when the MARHE combustion parameter is considered. Such a reduction in heat emission of PLA has only been achieved in the literature with a phosphorus-containing flame retardant content of significantly more than 20 wt%.[7]

It can be clearly seen in Figure 6b that the mass loss curve of the untreated PLA decreases sharply, leaving only a negligible amount of combustion residue, while the composites modified with the addition of APP and PSilAlg start to decompose earlier, but the mass loss rate is less steep and significant amount (>12%) of residue is left after combustion. The residual mass

Table 7. Combustion characteristics obtained by cone calorimeter tests.

	TTI [s]	PHRR [kW m^{-2}]	$PHRR_{time}$ [s]	MARHE [kW m^{-2}]	THR [MJ m^{-2}]	Residue [%]	TSP [m^2]	FRI [-]
PLA	89	284	334	177.3	76.5	0	0.27	1
PLA_APP	78	210	199	119.7	53.6	13.2	2.89	1.7
PLA_APP_1PSilAlg	69	186	157	90.6	51.2	12.8	1.7	1.8
PLA_APP_3PSilAlg	58	186	145	93.6	32.7	26.6	1.09	2.3
PLA_APP_5PSilAlg	62	177	137	75.6	28.9	35.7	0.98	3.0

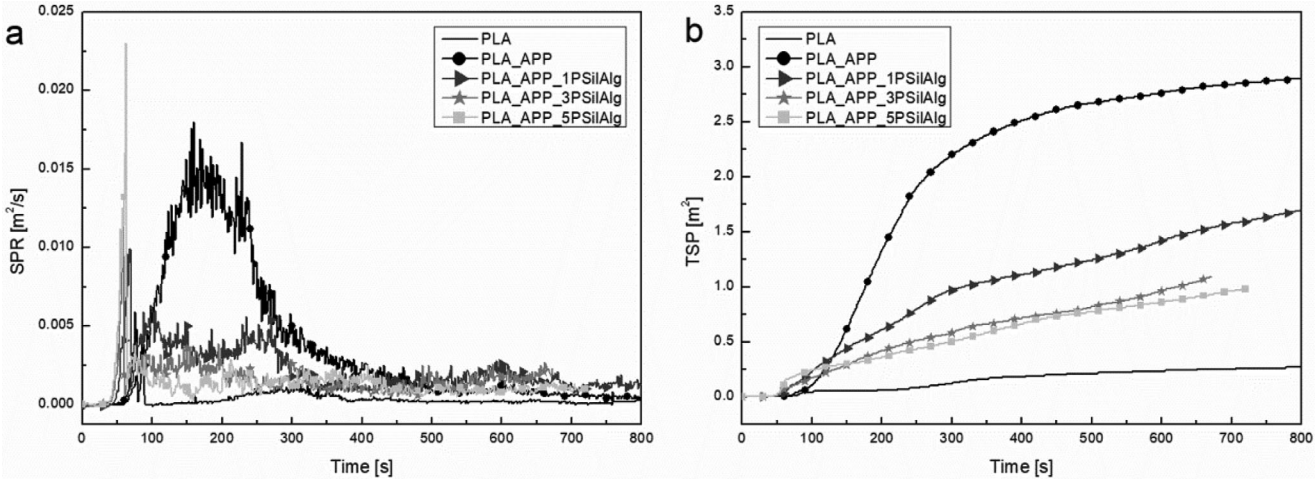

Figure 7. a) Smoke production rate and b) total smoke production of the flame retarded PLA composites.

after combustion with 15 wt% APP is ≈13%, while with the addition of 5 wt% PSilAlg, this value increases to ≈36%, which is likely a resulted by the effective charring of the modified alginate catalyzed by the high-valence phosphorus, as well as the ceramising effect caused by silicon. According to the calculated FRI values presented in Table 7, the use of PSilAlg as co-additive besides 15 wt% APP effectively increases the overall fire performance of the PLA composites. The addition of 5 wt% of PSilAlg increases the FRI of the 15 wt% APP-containing PLA composite from 1.8 to 3.0. In the literature, at similar loading of 16–20 wt% of phosphorus-based additives generally lower FRI values were reached in PLA matrix (FRI = 2.57 with 15 wt% APP/ 3 wt% HP-β-CD fiber additive;[34] FRI = 2.39 with 17 wt% APP/3 wt% lignin/1 wt% OMMT[35]) which reflects the excellent performance of the newly synthesized alginate based flame retardant additive.

Figure 7a presents the SPR of the composites. It can be observed that the addition of flame retardant additives to PLA increased the amount of emitted smoke in all cases but to a significantly different extent. This phenomenon is typical for P-containing compounds, whose mode of action in the gas phase is the blocking of chain reactions by radical capture and making the combustion of volatile compounds incomplete. In the condensed phase, however, the P-induced formation of a char layer can play an important role in the suppression of smoke production. Basically, the rate of these effects determines the overall effect of a phosphorus-flame retardant on the smoke release performance. It can be seen in Figure 7a, that the PLA sample containing only APP produced the highest amount of smoke during combustion, indicating the dominance of the flame-inhibiting mechanism and less effective condensed-phase action. The alginate-containing systems show greater smoke formation before ignition, but after ignition, a significant drop in SPR can be observed, and the values remain moderate until the end of combustion. Based on this behavior, an increased barrier effect of the chars formed from the PSilAlg-containing composites can be assumed, which applies even if only 1 wt% PSilAlg is added. Considering the TSP shown in Figure 7b, it can be seen that the addition of 1-3-5 wt% of PSilAlg reduced the total amount of emitted smoke by ≈41%, ≈62%, and ≈66%, respectively, compared to the sample containing only APP. The reduced smoke emission is likely related to the lower heat emission values, the reason for which is the higher yield and better quality of the formed carbonaceous protective layer.

3.2.5. Analysis of the Combustion Residues

Figure 8 shows the images of the combustion residues obtained after the cone calorimetric test. It can be clearly seen that the volume of charred residue increases with the amount of PSilAlg additive. The carbonaceous foam structures are coherent, and no defects are visible on them, which observation is consistent with their outstanding flame retardant efficiency evinced during the flame retardancy tests. Interestingly, small shiny particles were observed on the surface of the chars, which were subjected to further investigation by Raman spectroscopy (Section 3.2.5.2).

SEM images were taken of the surface of char residues, while the elemental composition of the combustion residues was characterized with EDS, by mapping both the inner part and the surface of the chars. As shown in **Figure 9**, the carbonaceous layers have a continuous structure, and there are blisters on their surface, the membranes of which become tighter as the PSilAlg content of the composites increases. According to the elemental content data presented in **Table 8**, the use of PSilAlg as co-additive besides APP resulted in a noticeable increase in the carbon content of the char residues. Such a coherent, more carbonaceous layer produced by catalytic carbonization can act as a better barrier against heat and oxygen diffusion and thus improve flame retardant and smoke suppression performance, as observed during cone calorimeter tests (Table 7). It can also be seen from Table 8 that the silicon-containing compounds are enriched on the surface of the char which may contribute to increased thermal stability of the fire-protecting layer.

The chemical composition of the combustion residues of the cone calorimeter tests was analyzed using the ATR-FTIR method. In the FTIR spectra presented in **Figure 10**, the peaks at 890,

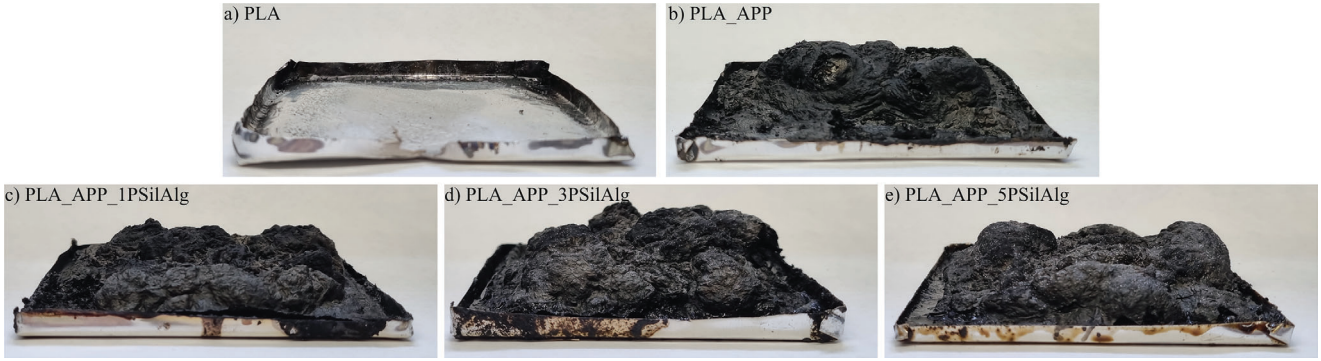

Figure 8. Combustion residues obtained after cone calorimeter tests.

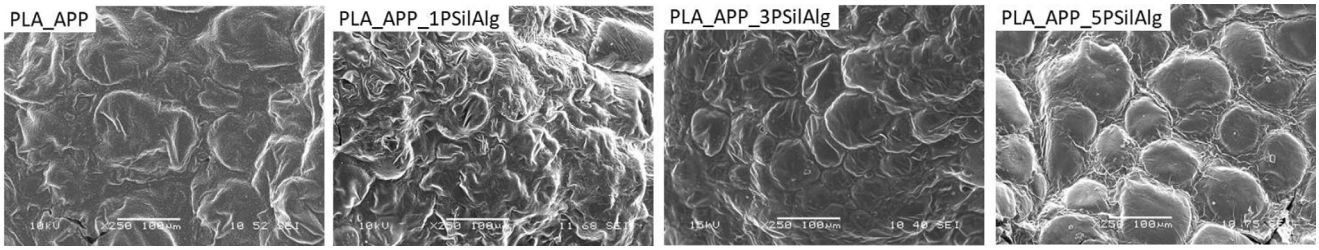

Figure 9. SEM images of the surface of char residue.

980, and 1147 cm^{-1} can be assigned to the stretching vibration of P—O—P, P—O—C, and P═O groups, respectively, indicating that the combustion residues contain pyrophosphate species that catalyze the char formation. Besides, the effective carbonization is indicated by the absorption peak at 1630 cm^{-1} attributed to the vibration of aromatic C═C bonds. New absorption peaks appeared in the FTIR spectra of the carbonaceous residues doped with PSilAlg compared to the spectrum of the residue corresponding to the only APP-containing sample. The peaks at 3640 and 875 cm^{-1} indicate the presence of CaO in the charred residues which is assumed to enhance the strength of the carbonaceous layer.[33] The sharp peak appearing at 1080 cm^{-1} in the spectra of samples containing PSilAlg corresponds to the Si—O—Si bond, while the peak at 1150 cm^{-1} indicates the presence of tetrahedral SiO_4. The vibrations of the Si—OH bond appear at 950 cm^{-1}, and the vibrations of the O—H bond in the Si—OH group appear at 3456 cm^{-1}. Based on these results, it was concluded that silicate crystals are formed from the PSilAlg additive under the conditions of combustion, which, due to their high reflectivity in the infrared region, can also contribute to the enhancement of the flame retardant effect.

Table 8. Elemental composition of char residues' inner part and surface.

	C [at%]		O [at%]		P [at%]		Si [at%]	
	inner	surface	inner	surface	inner	surface	inner	surface
PLA_APP	24.9	16.6	62.2	67.2	12.9	16.2	0	0
PLA_APP_1PSilAlg	30.4	44.3	49.4	43.4	19.5	12.0	0.7	0.3
PLA_APP_3PSilAlg	49.0	38.9	40.1	50.2	10.7	10.2	0.2	0.7
PLA_APP_5PSilAlg	66.4	42.4	28.2	46.1	5.3	10.6	0.1	0.9

The charred residue of the sample containing 15 wt% APP and 5 wt% PSilAlg was further analyzed by Raman spectroscopy. Raman spectra were collected using an objective with 20× magnification by focusing on a small, shiny particle, as shown in **Figure 11a**.

In Figure 11b, the band at 902 cm^{-1} was assigned to the Si—O— stretching in SiO_4 tetrahedron, while the sharp peak at 915 cm^{-1} is associated with non-bridging Si—O— bonds, and the peak at 1130 cm^{-1} indicates the appearance of SiO_2 units. The Raman spectroscopic analysis has confirmed that the glistening grains that can be observed with the naked eye on the surface of the

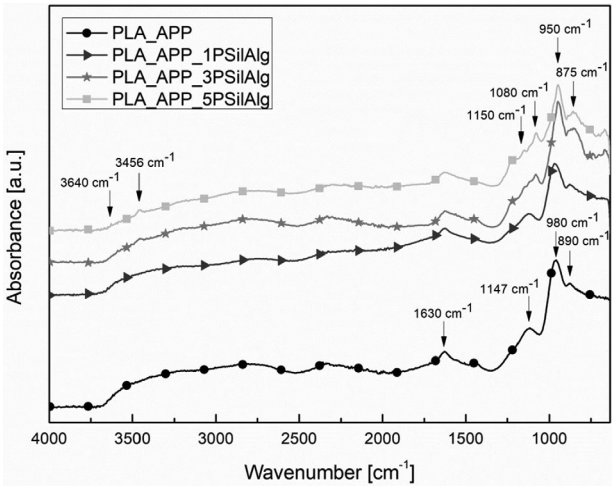

Figure 10. ATR-IR spectra collected from the combustion residues of the flame retarded PLA composites.

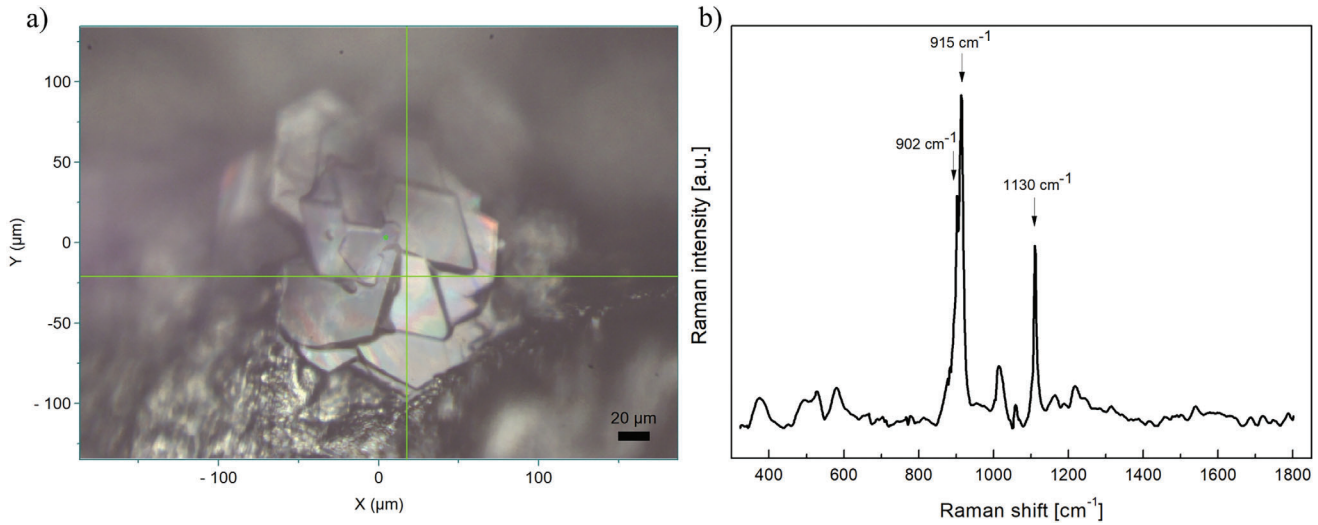

Figure 11. a) Optical microscopic image and b) Raman spectra collected from the combustion residue of the PLA composites with 15 wt% APP and 5 wt% PSilAlg.

charred combustion residues have a quartz-like, SiO_4 tetrahedral structure. The enhanced fire-protecting performance of the PSilAlg-containing composites, as observed in the cone calorimeter tests, is certainly largely attributed to this silicate-based inorganic layer that, upon heating, forms on the surface of the intumescent char by increasing thermal stability and heat reflectivity.

3.2.6. Further Characterisation of Flame Retarded PLA Composites

Differential scanning calorimetric analysis and dynamic mechanical characterisation of the PLA composites flame retarded with phosphorus and silicon modified alginate containing intumescent additive system are given as Supporting Information.

4. Conclusion

Alginate, a readily available natural polysaccharide was transferred into an effective flame retardant additive through reactive modification with a phosphorous-silane compound followed by calcium complexation. The modified alginate (PSilAlg) was obtained from addition reactions and using only water as solvent. TGA analyses revealed noticeable char-forming behavior of the PSilAlg compound without compromising thermal stability.

PSilAlg was found to be highly efficient in PLA matrix, even when used in small percentages (at 3–5 wt%); it resulted in a significant enhancement in the performance of a 15 wt% APP containing intumescent flame retardant system. The addition of 5 wt% PSilAlg increased the limiting oxygen index from 26.0, corresponding to the PLA_APP composite, to 34.0 vol%. A noticeable char-promoting effect of PSilAlg in PLA composites was revealed by TGA, PCFC, and cone calorimetric measurements, as well. After combustion at a heat flux of 35 kW m^{-2} under the cone heater, a considerable proportion of the PLA_APP_5PSilAlg composite, ≈36%, remained in the form of char. The formed carbonaceous fire-protecting layer proved to be prominent in suppressing

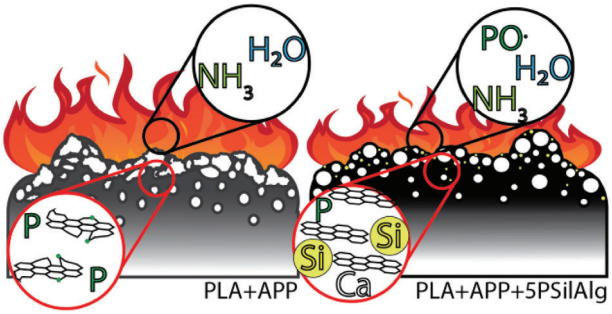

Figure 12. Schematic representation of the mechanism of APP_PSilAlg flame retardant system.

the production of heat (THR decreased by 46%) and smoke (TSP decreased by 66%). Comprehensive analyses (SEM-EDS, ATR-IR, and Raman spectroscopy) of the combustion residues revealed effective condensed-phase action of the PSilAlg additive, acting in parallel with the flame-inhibiting mechanism and reinforcing the solid-phase mechanisms of APP. The outstanding barrier efficiency of the intumescent chars formed from the PSilAlg-containing composites is attributed to their coherent, blister-like structure. Furthermore, on the surface of the formed polyaromatic carbonaceous layers silicate-based inorganic compounds are enriched which, together with calcium oxides, provide increased thermal and structural stability to the fire-protecting char (**Figure 12**).

Utilization of P–Si synergistic interaction is proposed as a promising way to endow biobased raw materials with enhanced flame retardant performance or other functionalities (e.g., modification of interfacial forces) and thus to make them more attractive to the market players in this field.

Supporting Information

Supporting Information is available from the Wiley Online Library or from the author.

Acknowledgements

This research was supported by The National Research, Development, and Innovation Fund of Hungary under Grant TKP2021-NVA-02 and 2019–1.3.1-KK-2019–00004 projects. Support from the ÚNKP-23-5-BME-417 New National Excellence Program of the Ministry for Culture and Innovation from the source of the National Research, Development and Innovation Fund was acknowledged. B.S. acknowledges the financial support received through the János Bolyai Scholarship of the Hungarian Academy of Sciences.

Conflict of Interest

The authors declare no conflict of interest.

Data Availability Statement

The data that support the findings of this study are available from the corresponding author upon reasonable request.

Keywords

alginates, chemical modifications, flame retardancy, intumescence, poly(lactic acid)

Received: May 27, 2024
Revised: July 4, 2024
Published online:

[1] L. Baochai, A. A. Bakar, Z. Mohamad, *Polym. Adv. Technol.* **2023**, *34*, 1435.
[2] W. S. Chow, E. L. Teoh, J. Karger-Kocsis, *eXPRESS Polym. Lett.* **2018**, *12*, 396.
[3] X. Wang, S. Wang, W. Wang, H. Li, X. Liu, X. Gu, S. Bourbigot, Z. Wang, J. Sun, S. Zhang, *Compos. B Eng.* **2020**, *183*, 07568.
[4] G. Fontaine, S. Bourbigot, *J. Appl. Polym. Sci.* **2009**, *113*, 3860.
[5] X.-Y. Pang, Y.-F. Meng, Y.-P. Xin, R. Chang, J.-Z. Xu, *Int. Polym. Proc.* **2021**, *36*, 367.
[6] X. Shan, J. Han, K. Jiang, J. Li, Xing, *Polym. Compos.* **2019**, *40*, 652.
[7] C. Réti, M. Casetta, S. Duquesne, S. Bourbigot, R. Delobel, *Polym. Adv. Technol.* **2008**, *19*, 628.
[8] R. Zhang, X. Xiao, Q. Tai, H. Huang, Y. Hu, *Polym. Eng. Sci.* **2012**, *52*, 2620.
[9] Q. Kong, B. Wang, Q. Ji, Y. Xia, Z. Guo, J. Yu, *Chin. J. Polym. Sci.* **2009**, *27*, 807.
[10] P. Zhu, C. Zhang, S. Sui, H. Wang, *Res. J. Text. Apparel.* **2009**, *13*, 1.
[11] J. Zhang, Q. Ji, X. Shen, Y. Xia, L. Tan, Q. Kong, *Polym. Degrad. Stab.* **2011**, *96*, 936.
[12] R. D. Mehta, *Text. Res. J.* **1974**, *44*, 825.
[13] Y.-J. Xu, L.-Y. Qu, Y. Liu, P. Zhu, *Carbohydr. Polym.* **2021**, *260*, 117827.
[14] N. Wu, F. Niu, W. Lang, M. Xia, *Carbohydr. Polym.* **2019**, *221*, 221.
[15] M. Lewin, *Polym. Adv. Technol.* **2001**, *12*, 215.
[16] X.-H. Shi, Q.-Y. Liu, X.-L. Li, A.-K. Du, J.-W. Niu, Y.-M. Li, Z. Li, M. Wang, D.-Y. Wang, *Polym. Degrad. Stab.* **2022**, *197*, 109839.
[17] J. Alongi, M. Ciobanu, G. Malucelli, *Carbohydr. Polym.* **2011**, *85*, 599.
[18] G. Brancatelli, C. Colleoni, M. R. Massafra, G. Rosace, *Polym. Degrad. Stab.* **2011**, *96*, 483.
[19] K. Bocz, B. Szolnoki, A. Marosi, T. Tábi, M. Wladyka-Przybylak, G. Marosi, *Polym. Degrad. Stab.* **2014**, *106*, 63.
[20] K. E. Decsov, B. Ötvös, G. Marosi, K. Bocz, *Polym. Degrad. Stab.* **2022**, *200*, 109938.
[21] J. Pallmann, Y. Ren, B. Mahltig, T. Huo, *J. Appl. Polym. Sci.* **2019**, *136*, 47794.
[22] W. Chen, Y. Liu, Y. Liu, Q. Wang, *J. Appl. Polym. Sci.* **2017**, *134*, 45552.
[23] J. Jiang, Y. Cheng, Y. Liu, Q. Wang, Y. He, B. Wang, *J. Mater. Chem. A Mater.* **2015**, *3*, 4284.
[24] B. Schartel, *Materials.* **2010**, *3*, 4710.
[25] B. Xu, Y. Liu, S. Wei, S. Zhao, L. Qian, Y. Chen, H. Shan, Q. Zhang, *Int. J. Mol. Sci.* **2022**, *23*, 11256.
[26] H. Vahabi, B. Kandola, M. Saeb, *Polymers.* **2019**, *11*, 407.
[27] Y. Yu, L. Xi, M. Yao, L. Liu, Y. Zhang, S. Huo, Z. Fang, P. Song, *iScience.* **2022**, *25*, 103950.
[28] Y. Zhang, P. Han, Z. Fang, *J. Appl. Polym. Sci.* **2018**, *135*, 46054.
[29] X. Jin, S. Cui, S. Sun, J. Sun, S. Zhang, *Polymers.* **2021**, 3513.
[30] M. Maqsood, G. Seide, *Polymers.* **2019**, *11*, 48.
[31] X. Wang, Y. Hu, L. Song, S. Xuan, W. Xing, Z. Bai, H. Lu, *Ind. Eng. Chem. Res.* **2011**, *50*, 713.
[32] Y. Li, B. Li, J. Dai, H. Jia, S. Gao, *Polym. Degrad. Stab.* **2008**, *93*, 9.
[33] Q. Huang, H. Xue, R. Dong, Y. Xue, X. Zhou, Z. Li, Q. Li, *Cellulose.* **2022**, *29*, 1759.
[34] K. Decsov, V. Takács, G. Marosi, K. Bocz, *Polym. Degrad. Stab.* **2021**, *191*, 109655.
[35] R. C. Martins, S. P. da Silva Ribeiro, R. S. V. Nascimento, M. A. C. Nascimento, M. Batistella, J. M. Lopez-Cuesta, *J. Appl. Polym. Sci.* **2022**, *139*, 52243.

